The Interaction between PEO-PPO-PEO Triblock Copolymers and Ionic Surfactants in Aqueous Solution Studied Using Light Scattering and Calorimetry

Jörgen Jansson,[†,$] Karin Schillén,[*,†] Gerd Olofsson,[†,§] Rodrigo Cardoso da Silva,[‡] and Watson Loh[‡,#]

Division of Physical Chemistry 1, Chemical Center, Lund University, P.O. Box 124, SE-221 00 Lund, Sweden, and Instituto de Química, Universidade Estadual de Campinas, Caixa Postal 6154, CEP 13083-970, Campinas, SP, Brazil

Received: June 26, 2003; In Final Form: October 8, 2003

Properties of nonionic triblock copolymers of poly(ethylene oxide) (PEO) and poly(propylene oxide) (PPO) ($EO_nPO_mEO_n$) in aqueous solution and their interaction with the ionic surfactants sodium dodecyl sulfate and hexadecyltrimethylammonium chloride have been investigated by static and dynamic light scattering, high sensitivity differential scanning, and isothermal titration calorimetry. The studied copolymers (denoted P123 and F127) have the same hydrophobic PPO central block ($m = 68$), but different length of the endblocks, $n = 20$ and 97. At 40 °C, the copolymers are associated into micelles with hydrodynamic radius of 9.8 nm (P123) and 12.5 nm (F127) composed of a hydrophobic PPO core and a water-swollen PEO corona. The different copolymer/surfactant systems have been investigated at a constant copolymer concentration of 1 wt % and with varying surfactant concentration up to about 120 mM. When ionic surfactants are added to the PEO−PPO−PEO block copolymer micellar systems, three concentration regimes are observed in the results from the complementary experimental techniques. At low surfactant concentrations (<1−2 mM), single surfactant molecules associate with the copolymer micelle forming a large copolymer-rich complex that becomes increasingly charged. The relaxation time distributions from dynamic light scattering are monomodal and the electrostatic interaction is evidenced in both the static and the dynamic light scattering results. In the intermediate surfactant concentration regime, two types of copolymer−surfactant complexes coexist, one large copolymer-rich complex and one small complex consisting of one or a few copolymer chains and rich in surfactant. This indicates a peel-off mechanism behind the disintegration of the copolymer micelles. The titration calorimetric data present an exothermic signal as the PPO blocks become rehydrated when the copolymer micelles break-up. At high surfactant concentrations, only the small surfactant-rich complexes are present in the systems.

Introduction

Studies of the interaction between nonionic water-soluble polymers and ionic surfactants are of significant interest because polymer−surfactant mixtures can be found in many industrial formulations such as paints and coatings, laundry detergents, cosmetic products, and pharmaceutical formulations. One type of interesting nonionic polymers are the triblock copolymers of poly(ethylene oxide) (PEO) and poly(propylene oxide) (PPO), PEO−PPO−PEO or $EO_nPO_mEO_n$ commonly known by the trade names Pluronics (BASF), Poloxamers (ICI), or Synperonics (ICI). PEO−PPO−PEO copolymers exist in different states of aggregation in aqueous solution depending on relative block sizes and on concentration and temperature. Their self-association behavior in water has attracted great attention in the literature; see, for example, the review articles, refs 1−7. Single molecular species (unimers) dominate at low temperatures and concentrations. At moderately high temperatures and concentrations, the PEO−PPO−PEO copolymers self-assemble to form micelles because of the limited and temperature-dependent solubility of the PPO block.[8−11] For these copolymers, owing to the polydispersity of the PPO and PEO blocks, the unimer-to-micelle transition occurs over a range in temperature and concentration, that is, with a much less sharp critical micelle temperature (CMT) and critical micelle concentration (CMC), compared to ordinary surfactants.[12−15] The structure of triblock copolymer micelles has been studied by a range of methods, where scattering techniques have been particularly successful.[4,14,16−23] Theoretical work and simulations on triblock copolymer systems made parallel to experimental investigations have also given valuable insight of micelle formation and structure.[10−13] The micelle consists of a core of mainly the hydrophobic PPO blocks with a low water content[24] surrounded by a water-swollen corona of PEO-blocks. At higher concentrations, the PEO−PPO−PEO copolymers can form a large number of various lyotropic liquid crystalline phases. Phase studies for several copolymers in aqueous solution have been carried out,[25−27] including systems containing a third component such as ionic-, nonionic-, cosurfactant, second solvent, or lipid.[28−33]

In the earlier studies on the association of sodium docecyl sulfate (SDS) and PEO−PPO−PEO copolymers, several methods such as nuclear magnetic resonance (NMR), fluorescence spectroscopy, various scattering techniques, and calorimetry have been used to investigate their interaction.[34−36] Extensive

* To whom correspondence should be addressed. E-mail: Karin.Schillen@fkem1.lu.se.
† Lund University.
‡ Universidade Estadual de Campinas.
$ E-mail: Jorgen.Jansson@fkem1.lu.se.
§ E-mail: Gerd.Olofsson@fkem1.lu.se.
# E-mail: wloh@iqm.unicamp.br.

10.1021/jp030792u CCC: $27.50
Published on Web 12/05/2003

studies of the F127/SDS system have been carried out using electromotive force measurements and calorimetry, in which binding isotherms, association mechanism, and synergistic behavior for the mixed micelles have been investigated.[37−40]

Recently, we published a study of the interaction between three triblock copolymers (F127, P123, and L121) and the ionic surfactants SDS and hexadecyltrimethylammonium chloride (CTAC) in dilute aqueous solution using calorimetric techniques as the main methods of investigation.[41] In this work, we have extended the investigation by using dynamic light scattering (DLS) and static light scattering (SLS) measurements. The purpose is to study in detail how the aggregation state of the copolymers is affected by charged surfactants. The paper is organized as follows: First, the DLS investigation on the dilute copolymer/water systems is presented, where the unimer-to-micelle transitions were studied with both concentration and temperature as variables. Thereafter, for each copolymer, the results of the combined light scattering and calorimetric studies of the interaction with either SDS or CTAC are discussed together with the effect of salt. Finally in the Conclusions, a model is given for how self-assembled structures of the copolymers change when ionic surfactants are introduced in increasing amount to the system.

Experimental Section

Materials. The PEO−PPO−PEO triblock copolymers have the average composition $EO_{20}PO_{68}EO_{20}$ (denoted P123, where P stands for "paste" and 3 for 30 wt % of PEO) and $EO_{97}PO_{68}$-EO_{97} (denoted F127, where F = "flakes" and 7 = 70 wt % of PEO) with a nominal molar mass of 5750 and 12 600 g mol^{-1}, respectively. They were a kind gift from BASF Corporation, Performance Chemicals, Mount Olive, New Jersey, and used without further treatment. The surfactant sodium dodecyl sulfate (SDS) was purchased from BDH, Analar Biochemical quality (>99%), and hexadecyltrimethylammonium chloride (CTAC) was purchased from Tokyo Chemical Industries (purity ≥ 95%). The purity of the surfactants was checked by DLS measurements, which showed an absence of contamination, that is, no aggregation below the critical micelle concentration (CMC) of the surfactants. NaCl was purchased from Riedel-de Haën, Pro analyze (purity ≥ 99.8%). The water used was treated with Millipore-Q water purification system. First stock solutions of the copolymer and surfactants were prepared and left to equilibrate overnight, the block copolymer solutions in a refrigerator at ca. 6 °C. The following day block copolymer/surfactant solutions were mixed and then left to equilibrate a second night in the refrigerator. All solutions were prepared by weight.

Copolymer Characterization. Because these copolymer samples are known to be heterogeneous and contain low-molar-mass components (homopolymers, diblock or triblock copolymers) that influence the self-association, it was of interest to characterize our samples.[14,16,22,42−44] We used gel permeation chromatography (GPC) with four columns coupled in series with tetrahydrofuran as solvent and an elution rate of 0.5 mL/min. For P123, we observed two nonresolved peaks in the chromatogram. The main peak is attributed to the triblock copolymer with the average composition $EO_{20}PO_{68}EO_{20}$. The second side peak (or shoulder) appearing at larger elution volume was assigned to low-molar-mass copolymer components, which made up about 10% of the injected material. The F127 sample gave a single slightly asymmetric peak in the GPC scan but with no shoulder, indicating that it is less heterogeneous than the P123 sample. This we also observed in the dynamic light scattering measurements, which indicated that most of these low-molar mass components in P123 are more hydrophobic than the main component and induce aggregation into larger sized aggregates ("clusters") below the critical micelle concentration.

Dynamic and Static Light Scattering. The setup for the dynamic light scattering (DLS) and static light scattering (SLS) measurements is an ALV/DLS/SLS-5000F, CGF-8F based compact goniometer system from ALV-GmbH., Langen, Germany. The light source is a CW diode-pumped Nd:YAG solid-state Compass-DPSS laser with symmetrizer from COHERENT, Inc., Santa Clara, California. It is operating at 532 nm with a fixed output power of 400 mW. A perfect vertical polarization is achieved using a Glan laser polarizer prism with a polarization ratio better than 10^5 in front of the cell housing. The scattering cells are immersed into a cylindrical quartz container, vat, which is filled with a refractive index matching liquid (toluene). The vat is positioned in a thermostated cell housing. The temperature of the vat can be varied from −12 to +140 °C and is controlled to ±0.01 °C by a F32 Julabo heating circulator. The goniometer has a range of scattering angles (θ) between 12° and 155°. The unpolarized scattered light is collected using a near-monomodal optical fiber and two matched photomultiplers that are put in a pseudo-cross-correlation arrangement. For DLS measurements using photon correlation spectroscopy, two multiple τ digital correlators, ALV-5000/E and ALV-5000/FAST Tau Extension, with a total of 320 exponentially spaced channels are employed to produce the time correlation function of the scattered intensity, $G^{(2)}(t)$ (auto or pseudo-cross), with an initial real sampling time of 12.5 ns. For the SLS and DLS measurements, about 1 mL of the cold solution was filtered through a sterile 0.20 μm Minisart filter (Sartorius, Germany) directly into the cylindrical light scattering cell. Prior to the measurements, the sample was equilibrated at room temperature for at least 20 min and thereafter for at least 30 min at the desired measuring temperature (usually 40 °C). This was to avoid any kinetic effects that appear if the block copolymer solution is exposed to temperature jumps over the critical micelle temperature (CMT) (data not shown). The copolymer content in the mixed copolymer/surfactant solutions was fixed to 1.0 wt % (= 1 wt % later in the text), if nothing else is mentioned. For the P123 solutions, the range in surfactant concentration was c_{SDS} = 0−98 mM and c_{CTAC} = 0−120 mM, and for the F127 solutions, the range was c_{SDS} = 0−92 mM and c_{CTAC} = 0−102 mM. In this study, no angular dependence of the static light scattering intensity was observed, and therefore, the SLS and DLS measurements presented below were performed at a constant scattering angle of θ = 90°, except for the DLS measurements shown in Figure 6.

Data Analysis. The measured quantity in DLS experiments is the time correlation function of the scattered intensity, $G^{(2)}(t)$.[45,46] The models used in the fitting procedures are expressed with respect to the normalized time correlation function of the electric field, $g^{(1)}(t)$, which is related to the measured intensity correlation function by Siegert's relationship:[47,48]

$$G^{(2)}(t) = B(1 + \beta|g^{(1)}(t)|^2) \quad (1)$$

where t is the lag time, B is the baseline, and β is the coherence factor (≤1) that takes into account deviations from ideal correlation and the experimental geometry. Here, the normalized form of the intensity correlation function, $g^{(2)}(t)$, is obtained directly from the software of the correlators during the DLS measurements with $g^{(2)}(t) - 1$ as the y-values.

For a solution containing monodisperse diffusing particles, $g^{(1)}(t)$ will be a single-exponential function with a single characteristic decay or relaxation time, τ. If the system is polydisperse and has a range of particle sizes, $g^{(1)}(t)$ will be multiexponential and may be expressed as a Laplace transformation of a distribution of relaxation times, $A(\tau)$:

$$g^{(1)}(\mathrm{t}) = \int_0^\infty \tau A(\tau) \exp(-t/\tau)\, \mathrm{d} \ln \tau \qquad (2)$$

where $\tau = \Gamma^{-1}$ and Γ is the relaxation rate that is used to calculate the translational mutual diffusion coefficient, D (see eq 3, below). The distribution of relaxation times is here written as $\tau A(\tau)$ for equal area representation [$\equiv \Gamma w(\Gamma)$ in the logarithmic scale].

The relaxation time distribution, $\tau A(\tau)$, is obtained by regularized inverse Laplace transformation (RILT) of the measured intensity correlation function using constrained regularization calculation algorithms, where the constraint is that the amplitudes of the relaxation times are positive. In the analyses in this work, algorithms of two commercial programs have been used: REPES,[48−51] incorporated in the GENDIST analysis package,[17,51] and RILT algorithm included in the ALV-5000/E software. In both these algorithms, the sum of the squared differences between experimental and calculated $g^{(2)}(t)$ functions is minimized and a regularization term is used. The regularizing term is adjustable through the "probability-to-reject term" α, and a value of 0.5 was chosen as standard in all the analyses presented here.[52] In most cases, we display the DLS results in the form of relaxation time distributions, that is, $\tau A(\tau)$ vs $\log(\tau/\mu s)$.

Differential Scanning Calorimetry. High-sensitivity differential scanning calorimetry (DSC) has been used to determine the transition temperatures and enthalpies of association of 1.0 wt % P123 solutions with varying surfactant concentrations both with and without NaCl (20 and 100 mM). The measurements were carried out using either a MC-2 or a VP-DSC high-sensitivity differential scanning calorimeter (MicroCal, Northhampton, MA.) in the temperature range 5−80 °C and a scanning rate of 54 °C/h. It uses 1.2 mL (or 0.54 mL for VP-DSC) total-fill cells with the sample solution in one cell and water (or aqueous NaCl solution) in the reference cell. The cold copolymer or copolymer−surfactant solutions were quickly transferred to the DSC cell kept at 5 °C, which was the starting temperature of the measurements, and they were equilibrated for 20 min before the temperature scan was started. After the scan was finished at 80 °C, the temperature was decreased to 5 °C, and the sample left to equilibrate for 20 min before a second scan was made. The second scan gave for all of the samples a curve that was identical to the curve for the first scan. Origin Software for DSC Data Collection and Analysis supplied by the manufacturer was used for instrument control, data acquisition, and analysis. The area under the peaks corresponds to the enthalpy of transition, ΔH_{tr}.

Isothermal Titration Calorimetry. The titration calorimetric measurements were performed using the 2277 TAM Thermal Activity Monitor system (Thermometric AB, Järfälla, Sweden). The experiments consisted of series of consecutive additions of concentrated surfactant solutions to the calorimeter vessel, containing initially 2.7 g of copolymer solution (1.0 wt %) or pure water (or aqueous NaCl solution) at 40 °C. The liquid samples were added in portions of 2−10 μL from a gastight Hamilton syringe through a thin stainless steel capillary tube. A microprocessor-controlled motor-driven syringe drive was used for the injections. The fast titration procedure was used with 6 min between each injection.[53] All experiments were repeated twice, and the reproducibility was good.

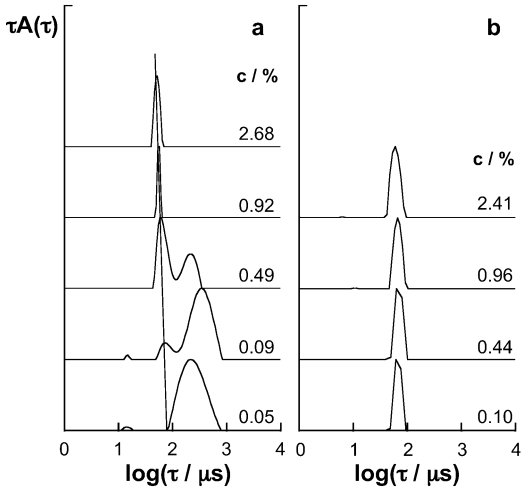

Figure 1. Relaxation time distributions obtained from inverse Laplace transformation of dynamic light scattering correlation functions at various concentrations for (a) P123 in water at 40 °C and (b) F127 in water at 40 °C. The peaks attributed to micelles are joined by a line. Measurements at $\theta = 90°$.

Results and Discussion

Block Copolymers in Water. *Dynamic Light Scattering.* DLS measurements were performed at 40 °C on P123 and F127 aqueous solutions with concentrations varying from 0.05 to 5.0 wt % of P123 and 0.1 to 2.4 wt % of F127 and at the scattering angle $\theta = 90°$. The copolymers are predominantly in micellar form, cf. ref 41, but at several of these concentrations, the DLS results indicate a complex aggregation behavior, as will be shown below. The relaxation time distributions [$\tau A(\tau)$ vs $\log(\tau/\mu s)$] obtained from the regularized inverse Laplace transformation of the measured intensity time correlation functions are presented for P123 in water in Figure 1a and for F127 in water in Figure 1b. In the P123 system, the relaxation distributions are monomodal as expected at concentrations from 0.9 wt % and above. The relaxation time of the single mode corresponds to the translational diffusion process of P123 micelles because the relaxation rate Γ ($= \tau^{-1}$) has a linear dependence on the square of the magnitude of the scattering vector, q^2, see eq 3. At P123 concentrations below 0.9 wt %, the relaxation time distributions are bimodal consisting of the micellar mode and an additional slower mode, which is broader. This mode is attributed to large clusters of unimers induced by more hydrophobic components in the sample (see Experimental Section). Although the clusters are not large in number, the cluster peak dominates the distribution because it is an intensity distribution, where the intensity is proportional to the 6th power of the radius. At higher concentrations, far above the critical micelle concentration (CMC), the hydrophobic components are incorporated into the hydrophobic core of the micelles and the relaxation time distribution becomes monomodal. This has also been observed for other PEO−PPO−PEO systems.[4,14,22] As may be seen in Figure 1a, a small peak at a fast relaxation time appears in the relaxation time distribution of the 0.09 wt % solution. This peak corresponds to the translational diffusion of single block copolymer P123 chains (unimers). At this concentration, unimers, micelles, and larger clusters coexist in the solution. At 0.05 wt %, the distribution is bimodal, consisting of the fast small unimer peak and a mode with slower relaxation time, which now includes the micellar mode. Although not

properly displayed in the present DLS experiments, it has been shown using DSC that P123 at 40 °C exists predominantly in the form of micelles in 0.05 wt % solution.[41] From the variation of the transition enthalpies, ΔH_{tr}, with concentration (see Table 1 in ref 41), we estimate a critical micelle concentration of 0.2×10^{-3} wt % at 40 °C. Hoffman et al. reported a CMC value of 0.3×10^{-3} wt % at 40 °C obtained from surface tension measurements,[26] and a value of (1×10^{-3})% (w/v) at 35 °C was determined by using UV−vis spectroscopy.[8] Hence, we conclude that the slow mode shown in the relaxation time distribution obtained for 0.05 wt % P123 in water is unresolved and a mixture of one micellar peak and one cluster peak.

Solutions of F127 containing between 0.1 and 2.4 wt % of copolymer give monomodal relaxation time distributions with micelles as single scattering objects. In some measurements with very good statistics, it was possible to extract an additional fast mode originating from the F127 unimers. However, the amplitude of this mode is 3 orders of magnitude less than the amplitude of the micellar mode and therefore not accurate enough for further investigation. It can be noticed that there is no indication of large clusters in the F127 system, which is consistent with the GPC results reported in the Experimental Section.

From the DLS data, the size of the micelles of P123 and F127 at 40 °C may be estimated. From the relaxation rate Γ, the apparent translational diffusion coefficient (D) at finite concentration can be calculated, given that $q \rightarrow 0$:

$$D = \left(\frac{\Gamma}{q^2}\right)_{q \rightarrow 0} \tag{3}$$

where q is the magnitude of the scattering vector; $q = 4\pi n_0 \sin(\theta/2)/\lambda$, where n_0 is the refractive index of the solvent, λ is the incident wavelength, and θ is the scattering angle. Here, D is obtained from the slope of $\Gamma = f(q^2)$.

The mutual diffusion coefficient measured in DLS contains both thermodynamic and hydrodynamic factors, which may be expressed in terms of concentration dependence:[54,55]

$$D = \frac{M(1-\phi)^2}{N_A f}\left(\frac{\partial \Pi}{\partial c}\right)_{T,p} = D_0(1 + k_d c + ...) \tag{4}$$

where M is the molar mass of the diffusing block copolymer micelle, N_A is the Avogadro's number, c is the copolymer concentration in mass/volume (or wt %), ϕ is the volume fraction of the copolymer, f is the concentration-dependent friction coefficient, and $(\partial\Pi/\partial c)_{T,p}$ is the inverse osmotic compressibility that takes into account the interparticle interactions in the system. With the use of virial expansions, eq 4 simplifies to a linear dependence in c with a slope k_d. D_0 is the free particle translational diffusion coefficient at infinite dilution from which a hydrodynamic radius (R_H) can be calculated using the Stokes−Einstein relationship: $R_H = kT/(6\pi\eta_0 D_0)$, where k is Boltzmann's constant, T is the absolute temperature, and η_0 is the viscosity of the solvent, which is water in this study.

Figure 2 presents D as a function of copolymer concentration for both P123 and F127 at 40 °C. Dividing the slopes, that is, k_d in eq 4, by the partial specific volume for each copolymer calculated from ref 56, we obtain a k_d' value of 2.36 for P123 and 7.10 for F127. These values may be compared to the k_d' for a hard sphere, which is 1.45.[57] The deviation from the hydrodynamic hard sphere behavior is due to the hydrated PEO corona of the micelles, which is larger in the case of F127, which has longer PEO chains. By extrapolation of the diffusion coefficients to zero concentration, the R_H values of the P123 and F127 micelles are found to be 9.8 and 12.5 nm. From repeated measurements on 1 wt % P123 in water, the standard deviation in the value of the apparent hydrodynamic radius R_H^{app} was less than 0.1 nm. The true R_H and the R_H^{app} values for both copolymers are in close agreement with those quoted in previous studies.[22,58,59] The small discrepancy that exists between the literature values is because different batches have been used in the different laboratories. Using the same procedure of analysis, we estimate the R_H of the large clusters in the P123 system to be around 40 nm, which is in the same order of magnitude as those observed in other PEO−PPO−PEO copolymer systems.[14]

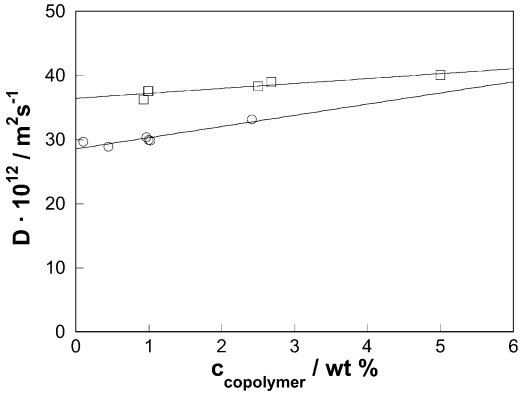

Figure 2. The diffusion coefficients of the block copolymer micelles at 40 °C as a function of copolymer concentration: P123 (□) and F127 (○).

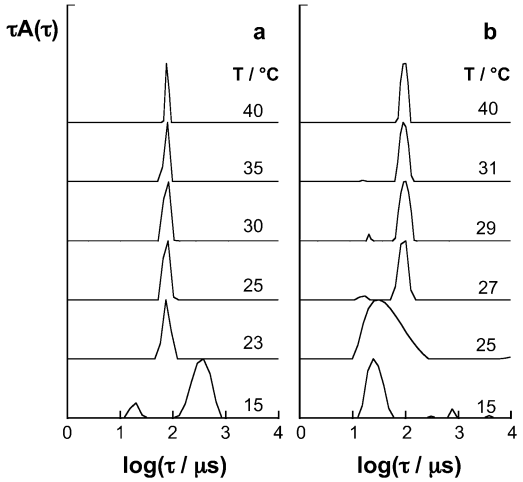

Figure 3. Relaxation time distributions at various temperatures for (a) 1.0 wt % P123 in water and (b) 1.0 wt % F127 in water. The data have been shifted by (T/η_0) on the $\log(\tau/\mu s)$ axis.

DLS measurements were also carried out on the fixed copolymer concentration of 1 wt % in water in the temperature range 15−40 °C to investigate the temperature dependence. The corresponding relaxation time distributions, shifted by a factor (T/η_0) to make them comparable, are presented in Figure 3a,b. At 15 °C, P123 and F127 exist as unimers, that is, the PPO block is soluble in water and hydrated. There are also larger clusters induced by the more hydrophobic components in the P123 solution at this temperature, whereas F127 does not show any large cluster peak in the relaxation time distribution. The fast mode ascribed to the diffusion of the unimers is rather broad, which is a reflection of the copolymer polydispersity. At 23 °C, micelles are the main scattering species in the P123 solution although only part of the sample is in micellar form. The distribution is monomodal and becomes narrower as the temperature increases indicating well-defined P123 micelles with

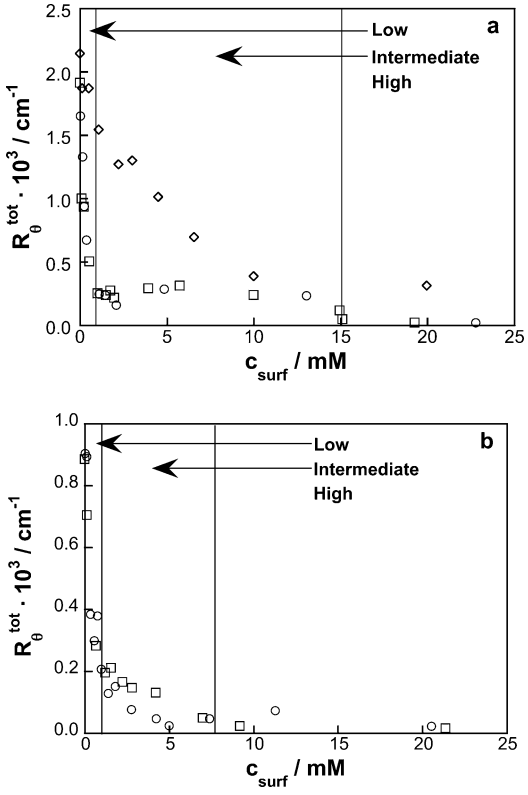

Figure 4. The total scattering intensity measured at $\theta = 90°$ as a function of surfactant concentration in 1.0 wt % copolymer solution at 40 °C for (a) the P123 system and (b) the F127 system: SDS (□); CTAC (○); CTAC in 100 mM NaCl (◇).

a narrow size distribution. The F127 system displays an asymmetric mode at 25 °C (Figure 3b). This peak contains unresolved contributions from the relaxation time of the F127 unimers and of the F127 micelles that start to form at this temperature. Above 25 °C up to 31 °C, the F127 distributions are bimodal. The fast mode with decreasing amplitude upon increasing temperature is ascribed to the translational diffusion of the unimers. The slow mode corresponds to the F127 micelles.

Block Copolymer−Surfactant Systems. The purpose of this work was to investigate the influence of addition of ionic surfactants, one anionic (SDS) and one cationic (CTAC), on the aggregation state of the block copolymers P123 and F127. The focus was to follow the changes in aggregation when surfactants interact with the block copolymer micelles using light scattering techniques supplemented by calorimetric techniques. Therefore, it was necessary to find a concentration and a temperature where the copolymer systems demonstrate an uncomplicated relaxation time distribution with micelles as the single scattering species. As seen in Figures 1 and 3, a copolymer concentration of 1 wt % measured at 40 °C was a suitable choice for our study. Furthermore, our present and previous DSC measurements show that the micelle formation of P123 and F127 is completed at 40 °C for 1 wt % solutions.[41]

Static and Dynamic Light Scattering. The total intensity of the scattered light of copolymer/surfactant solutions relative to the scattering intensity of toluene (the total Rayleigh ratio, R_θ^{tot}) was measured at 40 °C as a function of surfactant concentration without any solvent subtraction and at $\theta = 90°$. The results are shown in Figure 4a,b. Also included in Figure 4a are data points of P123/CTAC solutions containing 100 mM NaCl. The static light scattering intensity of the two P123/surfactant systems without NaCl exhibits three distinct regimes where the intensity changes, see Figure 4a. At low surfactant concentration (c_{surf} = 0.1−1 mM), there is a strong decrease in the scattered intensity. This effect originates mainly from the interparticle structure factor, which mirrors the electrostatic interaction between the P123 micelle−surfactant complexes as they become more and more charged when surfactant monomers bind noncooperatively to P123 micelles. In this concentration regime, we consider the change in the intensity due to a decrease in size of the P123 micelle−surfactant complex (i.e., the particle form factor) to be a minor effect. However, this is currently under investigation using small-angle X-ray scattering (SAXS).[60] At about 1 mM of surfactant, the total scattering intensity for the P123 systems reaches a plateau that extends up to about 15 mM, and we denote this range the intermediate surfactant concentration regime (Figure 4a). At higher surfactant concentrations, there is a final smaller intensity decrease, after which the intensity stays constant up to the highest surfactant concentrations investigated ($c_{surf} \approx 100-120$ mM). For P123, there is not a significant difference between the two surfactants.

The scattering intensity varied in a similar way with surfactant concentration in the F127/SDS and F127/CTAC systems with the exception that the changes in the F127/CTAC system occur at somewhat lower surfactant concentrations compared to the F127/SDS system as seen in Figure 4b. Finally, a constant low intensity value is reached, which continues up to $c_{surf} \approx 90-100$ mM. It is noticed that the intensity plateau at intermediate concentrations, which is seen in the P123 systems, is less pronounced in the F127 systems. For F127, the distinct decrease at concentrations below 1 mM of surfactant is followed by a more gradual change to lower intensities from ca. 1 mM and up to ca. 9 mM for SDS and up to ca. 5 mM for CTAC (both are lower concentrations than for P123). The observed difference between the copolymers reflects the lower *molar* concentration of F127, which is 0.79 mM compared to 1.7 mM for P123, because the PPO block length is the same for both copolymers. Comparable results from static light scattering, showing similar relative surfactant concentration regimes, have been observed for F127 systems containing SDS or tetradecyltrimethylammonium bromide.[35,37,38] Moreover, in a small-angle neutron scattering study on a F127/SDS system, it has been shown that at low surfactant concentrations, the aggregation number of the F127 micelle−SDS complex is constant, which supports the above statement concerning a constant form factor in this regime.[36]

The three different surfactant concentration regimes seen in the SLS measurements may be rationalized by simultaneously discussing the results from the DLS experiments that also were performed at 40 °C. A selection of relaxation time distributions of the 1 wt % P123/surfactant systems is shown in Figure 5a,b. Both systems display monomodal distributions, that is, single-exponential $g^{(2)}(t)$ functions, at low concentrations below 2 mM of surfactant. This mode corresponds to the translational diffusion process of the large P123 micelle−surfactant complex. As noticed, its relaxation time shifts toward faster times with increasing surfactant concentration (Figure 5a,b). This is mainly due to the electrostatic interaction between the increasingly charged complexes (see further discussion below). This part of the DLS data corresponds to the low surfactant concentration regime (0−1 mM) in the SLS experiments, where the scattering intensity expressed a dramatic decrease as shown in Figure 4a. Both of these effects can be ascribed to the electrostatic interaction between the P123 micelle−surfactant complexes. Because the relaxation time is affected, it was not possible to estimate a size in terms of R_H of the copolymer micelle−

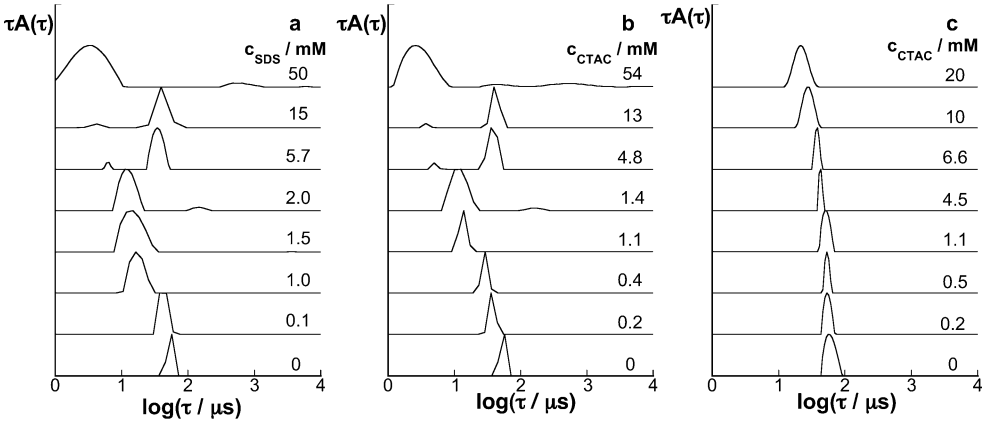

Figure 5. Selected relaxation time distributions for a 1.0 wt % P123 solution with varying surfactant concentrations at 40 °C: (a) SDS; (b) CTAC; (c) CTAC in 100 mM NaCl.

surfactant complexes. Therefore only changes in relaxation times are followed and commented upon when discussing the dynamic light scattering results. As previously mentioned, SAXS is currently utilized to determine the size of the complexes, and those results will be presented in a forthcoming publication.[60]

At $c_{surf} > 1$mM, the intermediate surfactant concentration regime is entered, which is represented by an intensity plateau in the SLS measurements (Figure 4a). This is also reflected in the DLS results, in which two relaxation modes are observed for the P123/SDS solutions containing between 5.7 and 15 mM SDS (Figure 5a). For the P123/CTAC solutions, the corresponding values are 4.8 and 13 mM (Figure 5b). The slow mode in the bimodal distributions is due to diffusion of a large P123 micelle−surfactant complex that corresponds to the single mode found at lower surfactant concentrations. The fast mode has a relaxation time close to that observed for pure micellar solutions of SDS [61] or CTAC (data not shown). It is therefore attributed to a small surfactant-rich complex that consists of cooperatively associated surfactants interacting with copolymer unimers. Thus, in this intermediate regime, two types of complexes coexist. The large copolymer-rich complex resembles the corresponding pure copolymer micelle, while the small complex is of the size of surfactant micelles. A similar observation has been described in a hydrophobic ethoxylated urethane (HEUR)/SDS system, where flowerlike HEUR micelles interact with SDS to form different complexes.[62] Furthermore, preliminary SAXS measurements present a significant change in the scattering curves in this concentration regime.[60]

In the intermediate concentration regime, in which bimodal relaxation time distributions were observed, angular dependent DLS was performed at 40 °C on a solution containing 1 wt % P123 and 7.7 mM CTAC (CTAC/P123 molar ratio = 4.5). The relaxation rates (Γ) for both the fast and the slow mode were measured as a function of q^2. The results are shown in Figure 6, in which the data have been fitted to eq 3. The linear relation of the relaxation rates confirms that both modes are due to translational diffusion processes, attributed to two different complexes, with the apparent mutual diffusion coefficients $D_{fast} = 59 \times 10^{-11}$ m^2 s^{-1} and $D_{slow} = 4.6 \times 10^{-11}$ m^2 s^{-1}. A growth in the amplitude of the fast mode was observed with increasing in P123 concentration at the same molar ratio (result not presented). Preliminary self-diffusion NMR data also indicate two different diffusion processes.[60]

An additional observation is that, in the low concentration regime between 1 and 2 mM surfactant, the single mode is broadened, which may indicate either a polydispersity of the large complexes or two unresolved peaks that are observed in the bimodal regime (see, for example, Figure 5b). Another observation is that the relaxation time of the slow mode is slower in the bimodal regime compared to the monomodal regime at lower surfactant concentrations (see, for example, Figure 5a). This shift in τ to slower times may arise from a change in the electrostatic interaction between the large copolymer micelle−surfactant complexes. A growth in size (τ is proportional to R_H^{app}) is not a reasonable explanation because we know from our present and previous calorimetric studies that the complexes disperse at high surfactant concentration.[41]

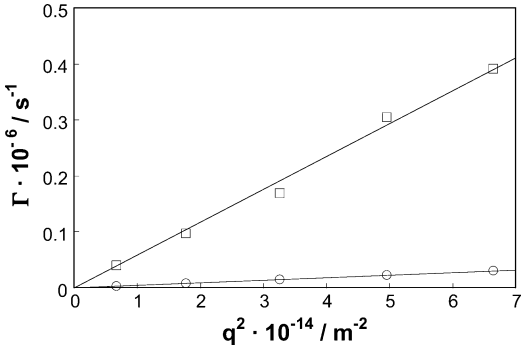

Figure 6. The relaxation rates for the fast (□) and the slow mode (○) as a function of the square of the magnitude of scattering vector for the 1.0 wt % P123 solution with 7.7 mM CTAC at 40 °C.

Finally, above ca. 20 mM of surfactant (23 mM for CTAC, 19 mM for SDS), the relaxation time distributions for both P123/surfactant systems become clearly monomodal again. This corresponds to the third surfactant concentration region, characterized by the lowest level in the scattering intensity curve (Figure 4a). Only small surfactant-rich complexes are left as scattering objects because the larger P123 micelle−surfactant complexes have disintegrated. In this high-surfactant region, it was difficult to obtain satisfying intensity correlation functions in the DLS measurements because of the low scattering intensity of the solutions. This fact is reflected by an increase in the peak widths in the relaxation time distributions, see Figure 5a,b, in addition to spurious peaks, which are artifacts from the Laplace inversion analysis. Furthermore, the width of the single mode may also be because the small complexes contain a varying number of P123 unimers before saturation is reached as was observed in the previously described fluorescence-quenching measurements on a similar block copolymer/SDS system.[34] Thus, the conclusion from these DLS measurements is that, at high surfactant concentrations, only small surfactant−copolymer complexes are present in solution with a size that resembles a surfactant micelle.

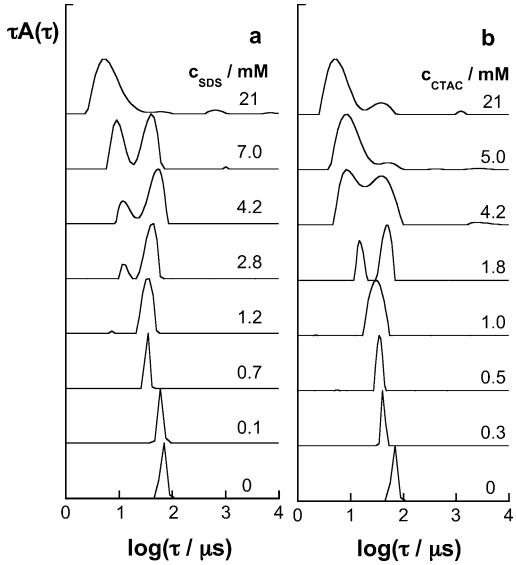

Figure 7. Selected relaxation time distributions for a 1.0 wt % F127 solution with varying surfactant concentrations at 40 °C: (a) SDS and (b) CTAC.

Examples of relaxation time distributions from DLS measurements on the F127/SDS and the F127/CTAC systems at a fixed copolymer concentration of 1 wt % and surfactant concentrations ranging between 0.1 and 100 mM are depicted in Figure 7a,b. Changes in the relaxation time distributions with increasing surfactant concentrations are similar to the changes observed for the P123 systems without salt (Figure 5a,b). The low concentration regime with one diffusive mode extends up to ca. 1 mM of surfactant. The distributions show a well-defined peak with a relaxation time that becomes shorter upon increasing surfactant concentration because of the electrostatic interaction. The translational diffusion of the charged F127 micelle−surfactant complex consisting of a F127 micelle with associated surfactant monomers gives rise to this mode. In this concentration range, the static light scattering intensity decreases strongly, which is seen in Figure 4b.

Above ca. 1−2 mM of surfactant, the relaxation time distributions for both F127/surfactant systems change to either a bimodal or a broad asymmetric unresolved monomodal appearance. The resolution of the modes depends on the statistics of the data collection. The bimodal regime ranges from 2.8 to 7.0 mM of SDS and from 1.4 to 4.2 mM of CTAC, see Figure 7a,b. The fast mode is due to the translational motion of a small surfactant-rich complex containing only a few F127 chains (similar as for the P123 systems). In a previous study, the coexistence of two complexes was also observed for the F127/SDS system with equimolar concentrations of SDS and NaCl at 25 °C in a small SDS concentration interval.[35] The relative amplitude for the fast mode increases in favor of the amplitude of the slow mode with increasing surfactant concentrations, which indicates an increase in number of small complexes. Finally, the slow mode diminishes above 7 mM SDS (Figure 7a) and ca. 4 mM CTAC (Figure 7b), and only one unresolved asymmetric mode at fast relaxation times is left. These surfactant concentrations correspond to the high surfactant concentration regime with low scattering intensity, as defined from the SLS experiments (Figure 4b). At these high surfactant concentrations, the large F127 micelle−surfactant complexes have broken up to give small surfactant-rich complexes. The ranges for the bimodal distributions are considerably narrower for F127 than for P123 probably due to the lower *molar* F127 concentration.

The effect of addition of simple salt, such as NaCl, to the P123/CTAC system was also investigated. The addition of 100 mM NaCl resulted in a much less drastic decrease in the scattering intensity in the low surfactant concentration regime than without salt as observed in Figure 4a. This is a direct effect of the reduced influence of the interparticle structure factor on the total scattering intensity due to the screening of the electrostatic repulsion between the large P123 micelle−CTAC complexes by the simple salt. Nevertheless, we cannot exclude that a minor size change of the complexes may occur in this low c_{CTAC} region. This would then be described in the form factor, which is the second contribution to the total scattering intensity. The influence of the change in the form factor is considered to be small, which is a statement that is currently under investigation by SAXS measurements on the P123/CTAC system.[60] However, at higher CTAC concentrations, the size of the complex decreases as seen below in the DLS measurements.

In Figure 5c, the results from DLS measurements on P123/CTAC solutions containing 100 mM NaCl are displayed. In this system, the relaxation time distributions show a well-defined single mode corresponding to the diffusion process of the complex for all CTAC concentrations investigated (up to 119 mM). For the P123/CTAC/NaCl solution containing 5 mM CTAC, a monomodal distribution is obtained, whereas the DLS data gave a bimodal distribution in the salt-free case (Figure 5b). This fact can be explained by that, in addition to influencing the interparticle interaction, the salt also screens the surfactant repulsion within the complexes. Furthermore, the pronounced shift toward faster relaxation times that was observed in the salt-free system was not found with salt present. This is the indirect evidence that the shift observed in the salt-free system is due to electrostatic interaction between the P123 micelle−CTAC complexes. Hence, as the electrostatic interactions have been screened, we may estimate the size of the diffusing particles in terms of an apparent hydrodynamic radius, R_H^{app}. R_H^{app} ranges from 10.6 nm (c_{CTAC} = 0 mM, P123 micelle) to 2.0 nm (c_{CTAC} = 119 mM, small CTAC−P123 complex). The results imply that instead of forming two coexisting complexes as in the salt-free case the size of the large P123-rich complex gradually decreases to the size of the small CTAC-rich complex upon increasing surfactant concentration.

P123/Surfactant Systems at Low Temperatures. The 1 wt % P123/surfactant systems were also investigated at lower temperatures. At 23 °C, the DLS results were similar to those at 40 °C for both surfactants and the behavior of the scattering intensity was about the same. At this temperature, the P123/water system displays a single micellar peak in the relaxation time distribution, as seen in Figure 3a. At 15 °C, P123 is below the critical micelle temperature, and no micelles are present in the solution. P123 unimers and unimer clusters are the two types of diffusing objects in the aqueous solution (Figure 3a). The SLS measurements performed on the 1 wt % P123/CTAC system at 15 °C show a decrease in the total scattering intensity upon increasing CTAC concentration up to 2 mM after which the intensity does not change up to high CTAC concentrations. The DLS measurements at 15 °C reveal the explanation for this behavior of the scattering intensity. The relaxation time distributions are bimodal at low CTAC concentrations (unimer + cluster). The amplitude of the cluster mode decreases gradually with increasing CTAC concentration and finally disappears at ca. 1 mM CTAC. Above this concentration, the distributions consist of one fast single mode, ascribed to the diffusion of a small CTAC−P123 complex. From these measurements, we may conclude that CTAC monomers first associate to the large

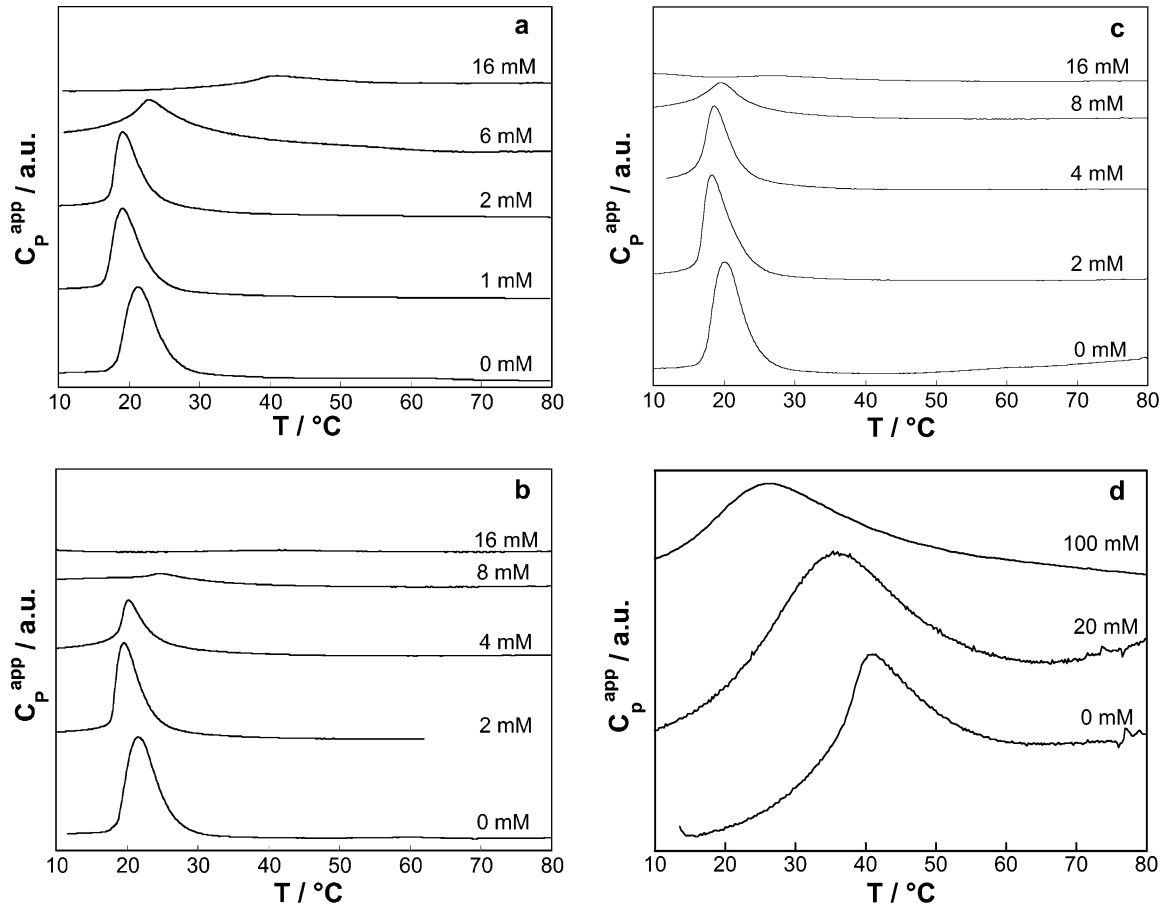

Figure 8. DSC curves of a 1.0 wt % P123 solution with varying surfactant concentrations: (a) SDS; (b) CTAC; (c) CTAC in 20 mM NaCl; (d) 15.6 mM SDS in 0, 20, and 100 mM NaCl.

hydrophobic clusters that disintegrate with increasing CTAC concentration. Thereafter, the surfactants interact with the P123 unimers to form the small surfactant-rich complex, which has been observed in similar studies.[37,38,39]

P123/Surfactant Systems at Low P123 Concentration. In 0.1 wt % P123 at 40 °C, unimers and large clusters coexist with micelles, as shown above in the relaxation time distributions obtained from DLS (Figure 1a). When small amounts of surfactants are added, the cluster mode is completely removed. This is valid for both SDS and CTAC. For example, already at 0.08 mM SDS, both the unimer and the cluster mode are replaced by a single mode that corresponds to the P123 micelle−SDS complex. Thus, addition of a small amount of surfactant can induce aggregation of the copolymer. This corresponds perfectly with the DSC measurements at low SDS concentrations presented in Figure 8a, where the temperature for the start of aggregation is lowered at the lowest surfactant concentrations. Thereafter, upon increasing surfactant concentration in 0.1 wt % P123, the DLS results show similar features as those for the 1 wt % P123 systems. Hence, the surfactant monomers associate preferentially with the clusters that contain hydrophobic copolymer components and cause the clusters to break-up. At the same time, the surfactant induces aggregation of unimers. Li et al. observed that SDS could promote F127 micelle formation at 3 °C below CMT for pure F127.[38,40]

Calorimetry. In a previous study, using differential scanning calorimetry (DSC) and isothermal titration calorimetry, we showed that block copolymer micelles of P123 and F127 and aggregates of the short PEO-winged L121 ($EO_5PO_{68}EO_5$) disintegrate upon addition of SDS and CTAC.[41] Eventually, a surfactant−copolymer complex is formed, probably of the same necklace type as PEO or PPO homopolymers with surfactant aggregates surrounded by polymers. In that study, the copolymer concentration was fixed to 0.1 wt % for the P123 system and to 1.0 wt % for the F127 system. To allow comparisons with results obtained from the light scattering experiments presented above, additional DSC and titration calorimetric measurements were therefore performed on the P123/surfactant systems with a fixed copolymer concentration of 1.0 wt %. The results from the DSC measurements for varying surfactant concentrations are shown in Figure 8a,b. The large peak at zero surfactant concentration depicts the micelle formation of the block copolymer P123. The enthalpy change, which is endothermic, is 477 kJ mol^{-1} for P123 and 366 kJ mol^{-1} for F127.[41] For both P123/surfactant systems, the peaks decrease upon addition of surfactant and vanish at about 15 mM SDS or about 8 mM CTAC. It is noticed that this decrease in the transition enthalpy, ΔH_{tr}, starts when the intermediate surfactant regime is entered (= the DLS bimodal regime). This indicates that fewer P123 unimers are involved in an aggregation process, where PPO dehydration takes place. The reason for the disappearance of the DSC peaks is that complexes with a large number of dehydrated PPO blocks no longer exist at high surfactant concentrations and a signal cannot be detected. Hecht et al. observed the same characteristic features in their studies.[35,36] A shift of the onset of aggregation toward higher temperatures is also clearly seen upon increasing surfactant content.

Addition of NaCl has a small but significant influence as seen in Figure 8c, in which the DSC measurements performed on P123/CTAC solutions containing 20 mM NaCl are shown. It is observed that the DSC peaks of the system with salt vanish at slightly higher surfactant concentration than those in the salt-

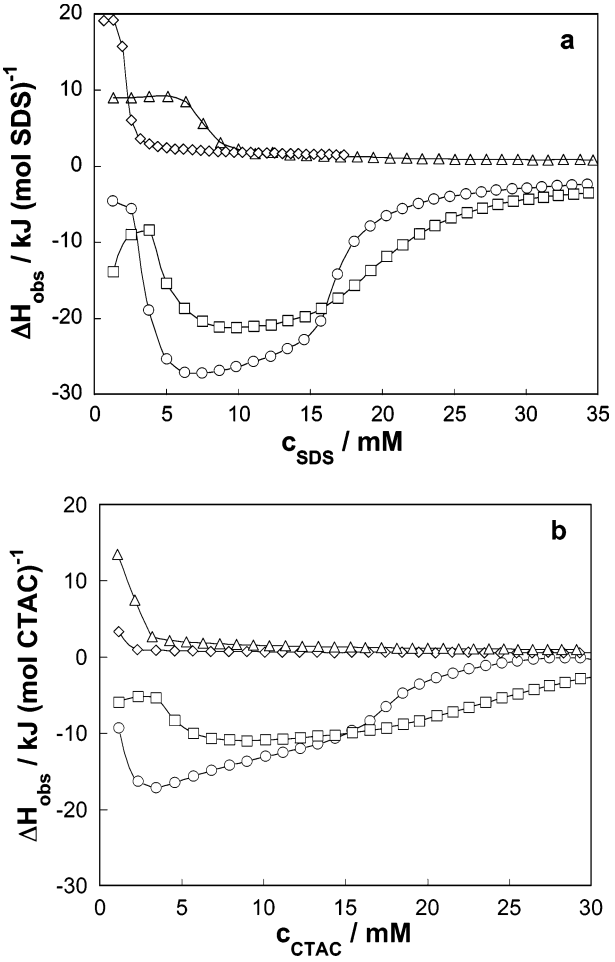

Figure 9. Titration curves for addition of surfactant into 1.0 wt % P123 solution at 40°C: (a) for SDS, 10 μL portions of 10 wt % SDS into P123 in water (○) and into P123 in 20 mM NaCl (□); (b) for CTAC, 10 μL portions of 5.0 wt % CTAC into P123 in water (○) and in P123 in 20 mM NaCl (□). Also included in panels a and b are the addition of surfactant solution to water (△) and to 20 mM NaCl (◇).

free case (compare panels b and c of Figure 8). This is a clear indication that the aggregation into a large P123 micelle−surfactant complex with many P123 unimers engaged in the process still ensues at higher surfactant concentrations if salt is present in the system. Figure 8d presents the DSC curves for a 1 wt % P123 solution containing 15.6 mM SDS and salt, either 20 or 100 mM NaCl, in comparison with the P123/SDS curve without salt. The presence of salt lowers the temperature of aggregation into a large P123 micelle−surfactant complex. Furthermore, the 100 mM trace shows that at 40 °C, the system is still aggregated into large P123 micelle−SDS complexes at this SDS concentration, which also was observed in the DLS measurements at 40 °C.

Isothermal titration calorimetric measurements were carried out at 40 °C with P123 concentration fixed to 1 wt %. These measurements are complementary to those performed previously by our group on 0.1 wt % of P123.[41] Figure 9a shows the results of addition of 10 μL portions of 10 wt % SDS solution to the 1 wt % P123 solution in addition to the curve for just adding SDS to water. Also included in the figure are the titration curves from addition of SDS to a P123 solution containing 20 mM NaCl. Figure 9b presents the curves from the addition of 5.0 wt % CTAC to P123 in water and in 20 mM NaCl solution, together with curves from addition of CTAC solution to pure water and to 20 mM NaCl solution. The results in water are first discussed.

Series of small injections (2.5 μL) of SDS to P123 in water gave exothermic enthalpy changes (ΔH_{obs}) that increased from -12 kJ mol^{-1} to a flat maximum of -4 kJ mol^{-1} between 1.4 and 2 mM (results not shown). Series of larger injections gave titration curves starting at the initial maximum as shown in Figure 9a. From 2 mM SDS, the observed enthalpy changes decreased to give a broad exothermic peak with a plateau at -27 kJ mol^{-1} between 5 and about 10 mM SDS. Then, the observed enthalpies slowly increased to about -22 kJ mol^{-1} at 15 mM SDS and then a steeper increase to about -8 kJ mol^{-1} at 19 mM SDS. Further addition of SDS gave a more gradual increase in ΔH_{obs}. Above 25 mM SDS, the observed enthalpies are small but still exothermic indicating continued interaction with the copolymer. The titration curves for addition of CTAC to P123 solutions show the same trends as can be seen in Figure 9b. In addition, the range up to 8 mM surfactant was studied in smaller steps with injection volumes of 2.5 μL (results not shown). ΔH_{obs} for the first injection of 0.29 mM was -1.6 kJ mol^{-1}. Further additions gave a steep decrease of the enthalpy values to a shallow minimum of -16 kJ mol^{-1} at around 3 mM. With increasing CTAC concentration, ΔH_{obs} becomes less exothermic and changes almost linearly up to 15 mM. Then, there is a steeper increase up to about 25 mM where the curve flattens out.

The exothermic peak that is observed in the titration calorimetry measurements for both surfactants reflects a rehydration of the PPO blocks of the copolymer chains as the P123 micelles break-up upon surfactant addition. In addition, these results show that in 1 wt % P123 the surfactants interact with the copolymer micelles already at the lowest concentration, 0.3 mM. The maxima in the titration curves indicate that the interaction changes character around 2 mM. We consider the exothermic minima in the titration curves to reflect the continued break-up of the copolymer micelles by peeling-off copolymer unimers to give small surfactant-rich complexes probably containing one or a few copolymer chains with hydrated PPO blocks. In these complexes, the PPO blocks of the copolymers are not as well-protected from water as they are in the block copolymer micelles. The presented titration curves for a 1 wt % P123 solution end before saturation is reached but after the P123 micelles are dispersed. We estimate that in a 1 wt % P123 solution saturation will not be reached until above 150 mM surfactant.[41]

The same conclusion of the final formation of small surfactant−copolymer complexes can be drawn for the F127 systems at high surfactant concentrations as well, see the calorimetric results of our previous work,[41] in addition to the DLS and SLS results displayed in Figures 7 and 4b, respectively. This has also been discussed in other investigations using various spectroscopic and calorimetric techniques.[34,36,37,39] The titration calorimetry data of the copolymer−surfactant systems presented here are closely similar to what was observed for the SDS−polyNIPAM microgel system.[63] At 40 °C, the microgel latex exists as compact particles containing only approximately two water molecules per isopropyl group. Addition of SDS to a microgel suspension gave a large exothermic peak in the titration curve, where the microgel took up water and swelled. Addition of SDS to the swollen microgel at 25 °C, where the polyNIPAM is fully hydrated, showed a typical calorimetric titration curve for a hydrophobic polymer. Thus, the hydration of the polyNIPAM is likely cause for the exothermic effect seen in their curve at 40 °C.

The addition of 20 mM NaCl reveals a clear effect in the isothermal titration calorimetric measurements on the P123/

surfactant systems at 40 °C (Figure 9a,b). For instance, the titration curve of SDS in salt solution displays the same features as that without salt but is shifted toward somewhat higher SDS concentrations. The first maximum is shifted from 2 mM to about 4 mM in the presence of salt, and the observed enthalpy changes are more exothermic, about -9 kJ mol^{-1} (Figure 9a). The beginning of the titration curve of CTAC in P123 solution containing 20 mM NaCl is closely similar to the curve for the SDS case (Figure 9b). After a maximum of about -5.2 kJ mol^{-1} at 2.3 mM CTAC, the curve decreases to a broad shallow exothermic minimum that is flatter and extends to higher CTAC concentrations than that in the salt-free solution (Figure 9b). Hence, these results confirm that the onset of the break-up process of the P123 micelles via the formation of a copolymer micelle−surfactant complex is pushed toward higher surfactant concentrations with salt present, which corresponds well with the results obtained from DSC (Figure 8b,c).

When we compare the results from the DLS and SLS experiments on P123/surfactant systems, shown in Figures 4a and 5, and the results from calorimetric measurements presented in Figures 8 and 9, the following observations are made: (1) The drastic decrease in the total scattering intensity takes place at low surfactant concentrations before the descent to the minima in the titration curves. The relaxation time distributions are monomodal. The peaks in the DSC curves indicate a small decrease in aggregation temperature. (2) At surfactant concentrations that give a minimum of the exothermic peak in the titration curves, the relaxation time distributions become bimodal and stay bimodal up to ca. 15 mM, at which there is a steeper increase in the observed enthalpy changes. At this concentration, the total scattering intensity decreases to the lowest level and the relaxation time distributions alter to single-modal. The peaks in the DSC curves decrease and vanish at about the same concentration. (3) The addition of salt tends to shift the changes in the calorimetric measurements to higher concentrations, that is, the presence of salt allows the binding of more surfactant to the copolymer micelles. The DLS measurements indicate that there is a gradual size decrease of the complex with increasing surfactant concentration as the electrostatic repulsion is screened.

Conclusions

The copolymer/ionic surfactant systems discussed in this work show the same basic features, and therefore, a model for how the self-assembled structures of the copolymers change when ionic surfactants are introduced to these systems may be presented.

When ionic surfactants are added to a PEO−PPO−PEO block copolymer micellar system, three concentration regimes are observed and expressed differently in the complementary experimental techniques that have been utilized in this study. These regimes are denoted the low, the intermediate, and the high surfactant concentration regime. At low surfactant concentrations ($<1-2$ mM), association with the block copolymer micelle occurs via noncooperative binding of surfactant monomers and a large copolymer-rich complex is formed, which becomes more charged as more surfactants are added to the system (*the low surfactant concentration regime*). The size of this complex is in the same range as the corresponding copolymer micelle. The binding of surfactant monomers can be considered as a solubilization of the hydrocarbon chains of the surfactants into the PPO core of the copolymer micelle. This regime is characterized by an increasing electrostatic interaction between the copolymer micelle−surfactant complexes, which can be lowered by addition of NaCl to the system. For copolymer concentrations of 1 wt %, the surfactant concentration of ca. 1 mM is an important concentration. At this concentration, all results from the different experimental techniques show changes, which demonstrates that a new process starts in the copolymer/surfactant systems. The scattering intensity reaches its plateau value, the DLS data changes from monomodal to bimodal distributions, titration calorimetric curves are either on the verge to the first descent toward the exothermic minimum or at the exothermic minimum and the DSC signal starts to decrease. We conclude that at this concentration the copolymer micelles start to disintegrate with the accompanied rehydration of the PPO blocks and a small surfactant-rich complex is formed (*the intermediate surfactant concentration regime*). In the small complexes cooperative surfactant aggregates interact with hydrated copolymer unimers. The small complexes coexist with the large copolymer micelle−surfactant complexes (a microphase separation) and grow in number until all unimers have been "peeled off" the large complex. At high surfactant concentrations, only the small surfactant-rich complexes are present in the system (*the high surfactant concentration regime*). The addition of NaCl to copolymer/surfactant systems suppresses the ability for the surfactants to break-up the copolymer micelles, and they can be preserved at higher surfactant concentrations than without salt.

Acknowledgment. Financial support from the former Swedish Natural Science Research Council (NFR) and the National Research Council (VR) (K. Schillén) and from FAPESP (W. Loh) are gratefully acknowledged. R. C. da Silva thanks CAPES (Coordenação de Aperfeiçoamento de Pessoal de Nível Superior) for the fellowship supporting his stay in Lund.

References and Notes

(1) Tuzar, Z.; Kratochvil, P. *Adv. Colloid Interface Sci.* **1976**, *6*, 201.
(2) Schmolka, I. R. *J. Am. Oil Chem. Soc.* **1977**, *54*, 110.
(3) Alexandridis, P.; Hatton, A. T. *Colloids Surf., A* **1995**, *96*, 1.
(4) Almgren, M.; Brown, W.; Hvidt, S. *Colloid Polym. Sci.* **1995**, *273*, 2.
(5) Chu, B.; Zhou, Z. Physical chemistry of polyoxyalkylene block copolymer surfactants. In *Nonionic Surfactants*; Nace, V. M., Ed.; Surfactant Science Series; Marcel Dekker: New York, 1996; Vol. 60, p 67.
(6) Alexandridis, P., Lindman, B., Eds. *Amphiphilic Block Copolymers: Self-Assembly and Applications*; Elsevier Science BV: Amsterdam, 2000.
(7) Kabanov, A. V.; Alakhov, V. Y. *Crit. Rev. Ther. Drug Carrier Syst.* **2002**, *19*, 1.
(8) Alexandridis, P.; Holzwarth, J. F.; Hatton, T. A. *Macromolecules* **1994**, *27*, 2414.
(9) Beezer, A. E.; Loh, W.; Mitchell, J. C.; Royall, P. G.; Smith, D. O.; Tute, M. S.; Armstrong, J. K.; Crowdhry, B. Z.; Leharne, S. A.; Eagland, D.; Crowther, N. J. *Langmuir* **1994**, *10*, 4001.
(10) Linse, P.; Malmsten, M. *Macromolecules* **1992**, *25*, 5434.
(11) Linse, P. *Macromolecules* **1993**, *26*, 4437.
(12) Linse, P. *Macromolecules* **1994**, *27*, 6404.
(13) Linse, P. *Macromolecules* **1994**, *27*, 2685.
(14) Brown, W.; Schillén, K.; Hvidt, S. *J. Phys. Chem.* **1992**, *96*, 6038.
(15) Reddy, N. K.; Fordham, P. J.; Attwood, D.; Booth, C. *J. Chem. Soc., Faraday Trans.* **1990**, *86*, 1569.
(16) Brown, W.; Schillén, K.; Almgren, M.; Hvidt, S.; Bahadur, P. *J. Phys. Chem.* **1991**, *95*, 1850.
(17) Schillén, K.; Brown, W.; Johnsen, R. M. *Macromolecules* **1994**, *27*, 4825.
(18) Chu, B. *Langmuir* **1995**, *11*, 414.
(19) Mortensen, K.; Pedersen, J. S. *Macromolecules* **1993**, *26*, 805.
(20) Goldmints, I.; Yu, G.-e.; Booth, C.; Smith, K. A.; Hatton, T. A. *Langmuir* **1999**, *15*, 1651.
(21) Mortensen, K.; Talmon, Y. *Macromolecules* **1995**, *28*, 8829.
(22) Nolan, S. L.; Phillips, R. J.; Cotts, P. M.; Dungan, S. R. *J. Colloid Interface Sci.* **1997**, *191*, 291.
(23) Lehner, D.; Lindner, H.; Glatter, O. *Langmuir* **2000**, *16*, 1689.
(24) Goldmints, I.; Von Gottberg, F. K.; Smith, K. A.; Hatton, T. A. *Langmuir* **1997**, *13*, 3659.

(25) Glatter, O.; Scherf, G.; Schillén, K.; Brown, W. *Macromolecules* **1994**, *27*, 6046.
(26) Wanka, G.; Hoffmann, H.; Ulbricht, W. *Macromolecules* **1994**, *27*, 4145.
(27) Noolandi, J.; Shi, A.-C.; Linse, P. *Macromolecules* **1996**, *29*, 5907.
(28) Zhang, K.; Lindman, B.; Coppola, L. *Langmuir* **1995**, *11*, 538.
(29) Holmqvist, P.; Alexandridis, P.; Lindman, B. *J. Phys. Chem. B* **1998**, *102*, 1149.
(30) Ivanova, R.; Alexandridis, P.; Lindman, B. *Colloids Surf., A* **2001**, *183*−*185*, 41.
(31) Alexandridis, P.; Yang, L. *Macromolecules* **2000**, *33*, 5574.
(32) Svensson, B.; Olsson, U.; Alexandridis, P. *Langmuir* **2000**, *16*, 6839.
(33) Bryskhe, K.; Schillén, K.; Löfroth, J.-E.; Olsson, U. *Phys. Chem. Chem. Phys.* **2001**, *3*, 1303.
(34) Almgren, M.; Van Stam, J.; Lindblad, C.; Li, P.; Stilbs, P.; Bahadur, P. *J. Phys. Chem.* **1991**, *95*, 5677.
(35) Hecht, E.; Hoffmann, H. *Langmuir* **1994**, *10*, 86.
(36) Hecht, E.; Mortensen, K.; Gradzielski, M.; Hoffmann, H. *J. Phys. Chem.* **1995**, *99*, 4866.
(37) Li, Y.; Xu, R.; Bloor, D. M.; Holzwarth, J. F.; Wyn-Jones, E. *Langmuir* **2000**, *16*, 10515.
(38) Li, Y.; Xu, R.; Couderc, S.; Bloor, D. M.; Holzwarth, J. F.; Wyn-Jones, E. *Langmuir* **2001**, *17*, 5742.
(39) Thurn, T.; Couderc, S.; Sidhu, J.; Bloor, D. M.; Penfold, J.; Holzwarth, J. F.; Wyn-Jones, E. *Langmuir* **2002**, *18*, 9267.
(40) Li, Y.; Xu, R.; Couderc, S.; Bloor, D. M.; Wyn-Jones, E.; Holzwarth, J. F. *Langmuir* **2001**, *17*, 183.
(41) da Silva, R. C.; Olofsson, G.; Schillén, K.; Loh, W. *J. Phys. Chem. B* **2002**, *106*, 1239.
(42) Gallet, G.; Carroccio, S.; Rizzarelli, P.; Karlsson, S. *Polymer* **2001**, *43*, 1081.
(43) Marinov, G.; Michels, B.; Zana, R. *Langmuir* **1998**, *14*, 2639.
(44) Linse, P.; Hatton, T. A. *Langmuir* **1997**, *13*, 4066.
(45) Berne, B. J.; Pecora, R. *Dynamic Light Scattering: with Applications to Chemistry, Biology, and Physics*, 2nd ed.; Dover Publications: New York, 2000.
(46) Young, R. J.; Lovell, P. A. *Introduction to Polymers*, 2nd ed.; Chapman & Hall: Cambridge, U.K., 1996.
(47) Siegert, A. J. P. *MIT Rad. Lab. Rep.* **1943**, No. 465.
(48) Stepánek, P. In *Dynamic Light Scattering*; Brown, W., Ed.; Oxford University Press: Oxford, U.K., 1993; p 177.
(49) Jakes, J. *Czech. J. Phys.* **1988**, *B38*, 1305.
(50) Nicolai, T.; Brown, W.; Johnsen, R. M.; Stepánek, P. *Macromolecules* **1990**, *23*, 1165.
(51) Johnsen, R. M.; Brown, W. In *Laser Light Scattering in Biochemistry*; Harding, S. E., Sattelle, D. B., Bloomfield, V. A., Eds.; The Royal Society of Chemistry: Cambridge, U.K., 1992; p 77.
(52) Jakes, J. *Collect. Czech. Chem. Commun.* **1995**, *60*, 1781.
(53) Bäckman, P.; Bastos, M.; Hallén, D.; Lönnbro, P.; Wadsö, I. *J. Biochem. Biophys. Methods* **1994**, *28*, 85.
(54) Vink, H. *J. Chem. Soc., Faraday Trans. 1* **1985**, *81*, 1725.
(55) Brown, W.; Nicolai, T. In *Dynamic Light Scattering*; Brown, W., Ed.; Oxford University Press: Oxford, U.K., 1993; p 272.
(56) Durchschlag, H.; Zipper, P. *Prog. Colloid Polym. Sci.* **1994**, *94*, 20.
(57) Pusey, P. N. Colloidal suspensions. In *Liquids, Freezing and Glass Transition*, 51st ed.; Hansen, J. P., Levesque, D., Zinn-Justin, J., Eds.; North-Holland: Amsterdam, 1991; Vol. 2, p 763.
(58) Wanka, G.; Hoffmann, H.; Ulbricht, W. *Colloid Polym. Sci.* **1990**, *268*, 101.
(59) Attwood, D.; Collett, J. H.; Tait, C. J. *Int. J. Pharm.* **1985**, *26*, 25.
(60) Jansson, J.; Schillén, K.; Nilsson, M.; Söderman, O.; Fritz, G.; de Campo, L.; Glatter, O., manuscript in preparation.
(61) Mazer, N. A.; Benedek, G. B.; Carey, M. C. *J. Phys. Chem.* **1976**, *80*, 1075.
(62) Dai, S.; Tam, K. C.; Jenkins, R. D. *J. Phys. Chem. B* **2001**, *105*, 10189.
(63) Wang, G.; Pelton, R.; Zhang, J. *Colloids Surf., A* **1999**, *153*, 335.